$MnSi_{1.7}$ nanoparticles embedded in Si: Superparamagnetism with collective behavior

Shengqiang Zhou (周生强),* Artem Shalimov, Kay Potzger, Manfred Helm, Jürgen Fassbender, and Heidemarie Schmidt
Institute of Ion Beam Physics and Materials Research, Forschungszentrum Dresden-Rossendorf, 01314 Dresden, Germany
(Received 24 August 2009; revised manuscript received 20 October 2009; published 25 November 2009)

The doping of Mn in Si is attracting research attentions due to the possibility to fabricate Si-based diluted magnetic semiconductors. However, the low solubility of Mn in Si favors the precipitation of Mn ions even at nonequilibrium growth conditions. $MnSi_{1.7}$ nanoparticles are the common precipitates, which show exotic magnetic properties in comparison with the $MnSi_{1.7}$ bulk phase. In this paper we present the static and dynamic magnetic properties of $MnSi_{1.7}$ nanoparticles. Using the Preisach model, we derive the magnetic parameters, such as the magnetization of individual particles, the distribution of coercive fields and the interparticle interaction field. Time-dependent magnetization measurements reveal aging and memory effects, qualitatively similar to those seen in spin glasses.

DOI: 10.1103/PhysRevB.80.174423 PACS number(s): 75.75.+a, 75.50.Pp

I. INTRODUCTION

Diluted magnetic semiconductors (DMSs) are attracting great interest because of their potential use for spintronics. GaAs:Mn has recently emerged as the most popular material for this new technology. However, Si-based DMS would be preferably used because of the availability of high quality, large-size, and low-cost wafers. More importantly, the fabrication of Si-based DMS is compatible with the mature microelectronics technique. Based on the Zener model, Dietl *et al.*[1] predicted carrier-mediated ferromagnetism if *p*-type conducting Si is doped with 5% Mn. Using density-functional theory, Wu *et al.*[2] demonstrated that interstitial Mn can be utilized to tune the magnetic properties of Si. Experimentally, various groups have reported the observation of ferromagnetism in Mn doped Si.[3–8] The reported Curie temperatures range from 200 to 400 K. However, the opinions concerning the origin of the observed ferromagnetism are very diverse. Using high-resolution spatially resolved techniques, comprehensive material characterization reveals the clustering of Mn-rich phases in Mn-implanted Si, namely, $MnSi_{1.7}$,[5,6,8–10] which is the energetically most favorable Mn-silicide phase.[11,12] Moverover, Mn-rich phases also form during pulsed laser annealing following Mn ion implantation into Si.[13] However, Mn precipitations in Mn-implanted GaAs are successfully suppressed.[14] Nevertheless, after considering the formation of $MnSi_{1.7}$ nanoparticles exotic magnetic properties have been observed. The magnetization per Mn is as large as $0.21\mu_B$/Mn, which is much larger than that ($0.012\ \mu_B$/Mn) of bulk $MnSi_{1.7}$.[5] Ko *et al.* suggested the existence of multifold contributions to the observed ferromagnetism according to their observation of Mn-rich and Mn-poor phases.[6,9] It is important to understand the dynamic magnetization of an ensemble of ferromagnetic nanoparticles due to its influence on technological applications. Spin-glass-like behavior has been observed in GaAs:Mn and Ge:Mn systems containing Mn-rich clusters.[15–17] Despite numerous publications on the structural and magnetic properties of $MnSi_{1.7}$ embedded in Si,[5–8,18] information of their dynamic properties is lacking. In this paper, we will present the static and dynamic magnetic properties of $MnSi_{1.7}$ nanoparticles. The magnetic parameters, such as the magnetization of individual particles, the distribution of coercive fields, and the interparticle interaction, are deduced using the Preisach model.[19,20] Time-dependent magnetization measurements reveal a spin-glass-like behavior.

II. EXPERIMENTAL METHODS

The Mn-implanted Si samples were prepared from commercially available, Czochralski grown single-crystal Si(001) wafers, which were *p*-type doped with a B concentration of 1.2×10^{19} cm^{-3}. Mn^+ ions were implanted at an energy of 300 keV with a fluence of 1.0×10^{16} cm^{-2}, which corresponds to a peak concentration of 0.8%, with a projected range (R_p) of 258 ± 82 nm. The samples were held at 350 °C during implantation to avoid amorphization. In order to reduce channeling effects, the angle between the sample surface normal and the incident beam was set to 7°. After implantation, rapid thermal annealing (RTA) was performed at a temperature of 800 °C for 5 min in a forming gas of N_2. Magnetic properties were analyzed using a superconducting quantum interference device magnetometer (Quantum Design magnetic property measurement system). In order to obtain the static and dynamic magnetic properties, we measured the magnetization depending on field, temperature and time.

III. RESULTS AND DISCUSSION

A. Static magnetic properties

The structural properties of the sample after rapid thermal annealing have been reported in Ref. 5. $MnSi_{1.7}$ nanoparticles are formed with the average diameter of 11 nm with a spherelike shape. We measured the magnetization of the sample by applying the field parallel or perpendicular to the sample surface and did not find any difference, which hints toward an isotropic magnetization. However, the same effect would be seen from a collection of anisotropic particles with randomly oriented easy axis. The *M-H* data for the sample with the field applied in the film plane is shown in Fig. 1. The linear diamagnetic background of the Si wafer has been subtracted for all shown data. The magnetization is normal-

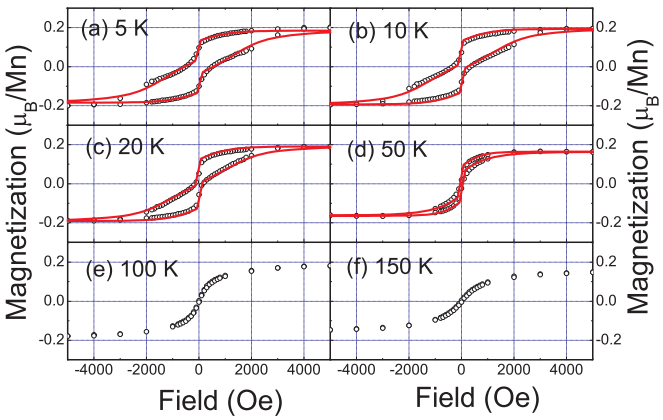

FIG. 1. (Color online) Hysteresis loops (open circles) measured in the temperature range from 5 to 150 K. (a)–(d) The solid curves are fittings using the Preisach model.

ized by the number of implanted Mn ions. It can be seen that the sample exhibits a hysteretic behavior with the magnetic remanence being 33% of the saturation magnetization at 5 K. With increasing temperature, both the coercivity (H_C) and remanence (M_R) drop rapidly. At 100 and 150 K, the coercivity and remanence are zero. This is the evidence for superparamagnetism. The blocking temperature lies between 50 and 100 K. Figure 2 shows the remanent magnetization measured from 5 to 200 K after shutting down the field of 10 000 Oe at 5 K. The remanence decreases rapidly with increasing temperature and falls to zero at around 80 K. The coercivity (inset of Fig. 2) exhibits a similar temperature dependence. Note that bulk $MnSi_{1.7}$ is reported to exhibit weak itinerant magnetism with an ordering temperature of 47 K and with a very low saturation moment of $0.012\mu_B$/Mn,[21] being much different from the $MnSi_{1.7}$ nanoparticles investigated here. In our samples, the largest magnetization is $0.21\mu_B$/Mn. Independently, Yabuuchi *et al.*[8] used slightly different implantation and annealing conditions and realized a maximum magnetization of $0.2\mu_B$/Mn. Both values are

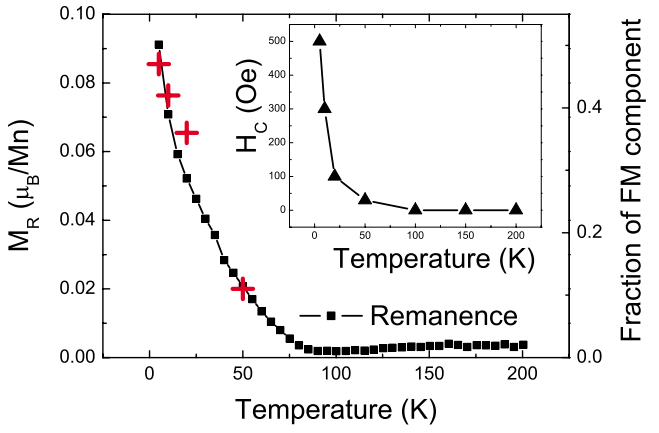

FIG. 2. (Color online) Measured temperature dependent remanence and coercivity (inset). Both drop to zero at the temperature around 80 K. The red crosses display the fraction of the ferromagnetic components obtained by fitting using the Preisach model. Both the remanence and the fraction of ferromagnetic component have the same temperature dependence.

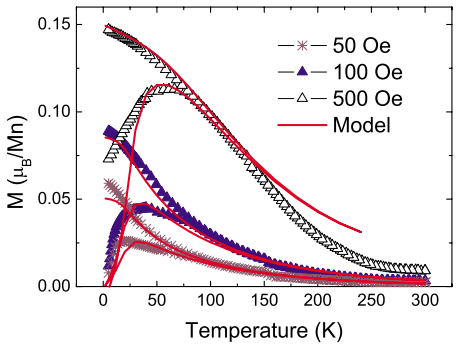

FIG. 3. (Color online) FC (upper branches) and ZFC (lower branches) *M-T* curves measured at different fields. The solid lines are fitting lines using the Preisach model.

much larger than for a bulk $MnSi_{1.7}$ crystal. Using first-principles calculation, Yabuuchi *et al.* clarified that the stoichiometry, strain and charge accumulation as well as the interface between $MnSi_{1.7}$ and Si strongly influence the magnetic properties of $MnSi_{1.7}$ nanoparticles.[7] These effects well account for the experimental observations.

The temperature dependent magnetization under zero-field cooling and field cooling was measured in the following way. The sample was cooled in zero field from above room temperature to 5 K. Then a field was applied and the zero-field-cooled (ZFC) magnetization curve was measured with increasing temperature from 5 to 300 K, after which the FC magnetization curve was measured in the same field from 300 to 5 K with decreasing temperature. Figure 3 shows the ZFC/FC magnetization curves measured at different fields. An irreversible behavior is observed in ZFC/FC curves. Such an irreversibility originates from the anisotropy barrier blocking of the magnetization orientation in the nanoparticles cooled under zero field. The magnetization direction of the nanoparticles is frozen in its initial state at high temperature, i.e., randomly oriented. At low temperature (5 K in our case), a magnetic field is applied. Some small nanoparticles with small magnetic anisotropy energy flip along the field direction, while the larger ones do not. With increasing temperature, the thermal activation energy together with the field also flips the larger particles. This process results in the increase of the magnetization in the ZFC curve with temperature. The peak of the ZFC curves, T_P, is considered as the average blocking temperature of the sample. A notable feature is the increase of T_P with increasing applied field. Such a field dependence of T_P has been observed in several magnetic nanoparticle systems, such as Fe_3O_4,[22] γ-Fe_2O_3,[23] ferritin,[24] and FePt.[25] The physical origin of this behavior is discussed concerning the size distribution of nanoparticles[25] and the interparticle interaction.[24]

We analyzed the experimental curves using simulations based on the Preisach approach[19,26] and derived the key magnetic parameters of $MnSi_{1.7}$ nanoparticles, namely, the magnetization of individual particles and the distributions of coercive and interparticle interaction fields. The temperature dependence of the parameters p describing the magnetic properties of the nanoparticles is usually expressed by the critical temperature T_C and the critical exponent γ,

TABLE I. Best fit Preisach parameters.

T_C (K)	μ_0 (emu)	N (cm^{-2})	Γ	Γ_c	H_{c0} (Oe)	σ_{c0} (Oe)	Γ_c'	σ_{i0} (Oe)	Γ_i
320	4.0×10^{-17}	4.3×10^{11}	0.6	0.6	1500	2000	0.6	200	0.1

$$p = p_0(1 - T/T_C)^{\gamma}, \tag{1}$$

with p (the subscript 0 denotes the parameters at 0 K) substituted by the mean magnetic moment μ of an individual cluster (where $\gamma=\Gamma$), the mean coercivity $H_C(\gamma=\Gamma_c)$, or the dispersions $\sigma_i(\gamma=\Gamma_i)$ and $\sigma_c(\gamma=\Gamma_c')$ of the interparticle interaction and coercive field, respectively. Long-range interaction field was equal to zero. The fitting parameters are shown in Table I.

Figure 4 shows a representative fitting of the hysteresis measured at 20 K. Two components contribute to the measured magnetization: a superparamagnetic (SP) component and a ferromagnetic (FM) component with a large coercive field of 1100 Oe. Note that the modeled coercivity of the FM component is larger than that shown in the inset of Fig. 2, and the modeled and the measured remanence are the same. The smaller coercivity seen in the measured hysteresis is due to the superposition of the FM and SP components. The fraction of the ferromagnetic component rapidly decreases with increasing temperature and is plotted in Fig. 2. It is worth to note that using the same set of fitting parameters we are able to fit the experimental curves measured at different temperatures (see Fig. 1).

The average magnetic moment of individual particles μ_0 (at 0 K) computed from the fitting is 4.0×10^{-17} emu (around $4300\mu_B$). The average diameter of $MnSi_{1.7}$ particles in this sample is around 11 nm.[5] In one particle there are approx. 21 000 Mn atoms, and we obtain $0.204\mu_B$/Mn. This value is in a good agreement with the experiment ($0.21\mu_B$/Mn). In the work by Yabuuchi *et al.*,[8] the samples with the same Mn fluence were annealed at different temperatures to tune the size of $MnSi_{1.7}$ particles. The ferromagnetism strongly depends on the average particle diameters and is maximized after annealing at 750 °C. This annealing temperature resulted in an average diameter of 10 nm for

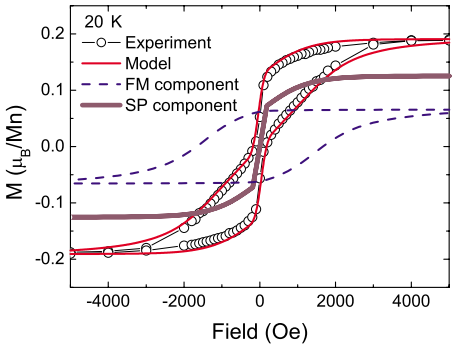

FIG. 4. (Color online) Fitting of the hysteresis loop measured at 20 K by the Preisach model. The SP and FM components are shown in the figure separately.

$MnSi_{1.7}$ particles. By the two experimental works[5,8] and our fitting using the Preisach approach, we confirm that the ferromagnetism in $MnSi_{1.7}$ particles strongly depends on their diameters; i.e., the exotic ferromagnetism in $MnSi_{1.7}$ particles is mainly a size effect.[7]

The ferromagnetic component has a large coercive field of 1500 Oe at 0 K, while the interparticle interaction is weak. Note that σ_i is around 200 Oe and much smaller than the coercive field (Table I). These features are important for practical applications. Using the same fitting parameters, the ZFC/FC curves are also well fitted as shown in Fig. 3. Importantly, the fitting reproduces the field dependence of T_P in the ZFC curves well. Indeed, Song *et al.* discussed the influence of the interparticle interaction using the Preisach model.[27] In the limit of weak interactions T_P increases monotonically with applied fields, while in the limit of strong interactions T_P decreases monotonically with applied fields. Therefore, we attribute the increase in T_P at larger fields to the weak interaction between $MnSi_{1.7}$ particles.

B. Dynamic magnetic properties

To obtain the dynamic magnetic properties of the system, we performed time-dependent measurements. The time-dependent thermoremanent magnetization (TRM) was measured below the blocking temperature. TRM is measured by cooling the sample in an applied field from an initial temperature above any spin-glass transition to some final temperature, decreasing the field to zero and observing the decaying remanent magnetization $[M_r(t)]$. In our case, TRM data were taken after cooling from 300 to 5 K and 20 K, respectively, in an applied field of 100 Oe.

For superparamagnetic nanoparticles, the magnetization decay is usually exponential to first order, such that one should observe a single relaxation rate approximation,[28]

$$M_r(t) = M_0 e^{-t/\tau} + C, \tag{2}$$

where M_0 is the initial magnetization, τ is the relaxation time and C is a constant. If the superparamagnetic nanoparticles undergo collective behavior due to direct dipole-dipole interaction or a large particle-size distribution, a stretched-exponential form is expected,[16]

$$M_r(t) = M_0 e^{-(t/\tau)^b} + C, \tag{3}$$

where b affects the relaxation rate of the glassy component. Figure 5 shows the TRM time decays at 5 and 20 K. The stretched-exponential relaxation fits better to the experimental data. The fitted parameters of τ and b are in the typical range of a spin-glass system.[16]

In order to further confirm the glass behavior of the system, we also performed history-dependent magnetic memory

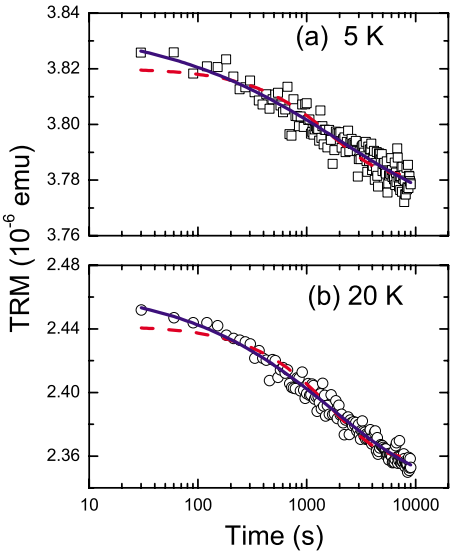

FIG. 5. (Color online) TRM time decays of the field-cooled magnetization ($H=100$ Oe) at (a) 5 and (b) 20 K. Scattered symbols are experimental data. Solid lines (blue) are stretched-exponential fits with parameters of $\tau=2120$ s and $b=0.44$ at 5 K, and $\tau=1806$ s and $b=0.53$ at 20 K. Dashed lines (red) are first-order exponential fits with parameters of $\tau=1721.2$ s at 5 K and $\tau=1720.5$ s at 20 K.

measurements using the cooling and heating protocol suggested by Sun *et al.*[29] We cooled the sample at 100 Oe and recorded the magnetization during cooling but temporarily stopped at $T=50$ and 30 K for a period of 2 h. During the waiting period, the field was switched off. After the stop, the 100 Oe field was reapplied and cooling and measuring were resumed. The temporary stop resulted in a steplike $M(T)$ curve (solid squares in Fig. 6). After reaching the lowest temperature 5 K, the sample was heated back in the same field, and the magnetization was recorded again. The $M(T)$ curve during this heating also has a steplike behavior at the stop temperature of 30 and 50 K, then recovers the previous $M(T)$ curve measured during cooling. The system remembers its thermal history.

The observed memory effect as well as the relaxation phenomena show qualitative similarities to the spin-glass behavior. Two explanations have been suggested.[30] The first one is a broad distribution of blocking temperatures originating from the distribution of the anisotropy energy barriers. Another explanation is the strong dipolar interaction between nanoparticles, which frustrates the nanomagnetic moments, and slows down their relaxation. Our observations support the first model. First of all, using the Preisach model we

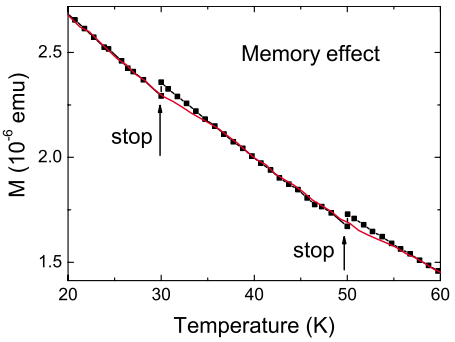

FIG. 6. (Color online) Temperature-dependent memory effect in the dc magnetization. The solid squares are measured during cooling in a field of 100 Oe at the same rate but with a stop of 2 h at 50 and 30 K, respectively. The field is cut off during stop. The solid line is measured with continuous heating at the same rate after the previous cooling protocol.

derived a small interaction between $MnSi_{1.7}$ nanoparticles. Second, the size of $MnSi_{1.7}$ nanoparticles approximately amounts to 11 ± 5 nm according to the TEM observation as shown in Ref. 5. The spin-flip time for magnetic particles depends exponentially on the particle size. Therefore, even a small distribution of the particle size could give a broad range of relaxation times. Therefore, the observed spin-glass-like behavior is attributed to the broad distribution of particle sizes, i.e., of anisotropy energy barriers.

IV. CONCLUSIONS

Static and dynamic magnetic properties of Mn-implanted Si were investigated. The magnetic properties of Mn-silicide nanoparticles can be well explained using the Preisach model. We found that there are two components (superparamagnetic and ferromagnetic fractions) contributing to the magnetism. The fraction of the ferromagnetic component decreases with increasing measurement temperature. The interaction between the magnetic nanoparticles is weak. Therefore, the superparamagnetism blocking temperature increases monotonically with applied field. Time-dependent measurements, i.e., relaxation and memory effect, support a spin-glass-like behavior in the investigated material system, which results from the size distribution of $MnSi_{1.7}$ nanoparticles.

ACKNOWLEDGMENTS

The author (S.Z.) acknowledges the financial funding from the Bundesministerium für Bildung und Forschung (Contract No. FKZ13N10144), and A.S. wants to thank the Deutsche Forschungsgemeinschaft (Contract No. PO1275/2-1, "SEMAN").

*s.zhou@fzd.de

[1] T. Dietl, H. Ohno, F. Matsukura, J. Cibert, and D. Ferrand, Science **287**, 1019 (2000).

[2] H. Wu, P. Kratzer, and M. Scheffler, Phys. Rev. Lett. **98**, 117202 (2007).

[3] F. M. Zhang, X. C. Liu, J. Gao, X. S. Wu, Y. W. Du, H. Zhu, J. Q. Xiao, and P. Chen, Appl. Phys. Lett. **85**, 786 (2004).

[4] M. Bolduc, C. Awo-Affouda, A. Stollenwerk, M. B. Huang, F. G.

Ramos, G. Agnello, and V. P. LaBella, Phys. Rev. B **71**, 033302 (2005).
[5] S. Zhou, K. Potzger, G. Zhang, A. Mücklich, F. Eichhorn, N. Schell, R. Grötzschel, B. Schmidt, W. Skorupa, M. Helm, J. Fassbender, and D. Geiger, Phys. Rev. B **75**, 085203 (2007).
[6] V. Ko, K. L. Teo, T. Liew, T. C. Chong, M. MacKenzie, I. MacLaren, and J. N. Chapman, J. Appl. Phys. **104**, 033912 (2008).
[7] S. Yabuuchi, H. Kageshima, Y. Ono, M. Nagase, A. Fujiwara, and E. Ohta, Phys. Rev. B **78**, 045307 (2008).
[8] S. Yabuuchi, Y. Ono, M. Nagase, H. Kageshima, A. Fujiwara, and E. Ohta, Jpn. J. Appl. Phys. **47**, 4487 (2008).
[9] V. Ko, K. L. Teo, T. Liew, T. C. Chong, T. Liu, A. T. S. Wee, A. Y. Du, M. Stoffel, and O. G. Schmidt, J. Appl. Phys. **103**, 053912 (2008).
[10] C. Awo-Affouda, M. Bolduc, M. B. Huang, F. Ramos, K. A. Dunn, B. Thiel, G. Agnello, and V. P. LaBella, J. Vac. Sci. Technol. A **24**, 1644 (2006).
[11] Z.-Q. Zou, H. Wang, D. Wang, Q.-K. Wang, J.-J. Mao, and X.-Y. Kong, Appl. Phys. Lett. **90**, 133111 (2007).
[12] D. Wang and Z.-Q. Zou, Nanotechnology **20**, 275607 (2009).
[13] N. Peng, C. Jeynes, M. J. Bailey, D. Adikaari, V. Stolojan, and R. P. Webb, Nucl. Instrum. Methods Phys. Res. B **267**, 1623 (2009).
[14] M. A. Scarpulla, O. D. Dubon, K. M. Yu, O. Monteiro, M. R. Pillai, M. J. Aziz, and M. C. Ridgway, Appl. Phys. Lett. **82**, 1251 (2003).
[15] W. Z. Wang, J. J. Deng, J. Lu, B. Q. Sun, and J. H. Zhao, Appl. Phys. Lett. **91**, 202503 (2007).
[16] C. Jaeger, C. Bihler, T. Vallaitis, S. T. B. Goennenwein, M. Opel, R. Gross, and M. S. Brandt, Phys. Rev. B **74**, 045330 (2006).
[17] S. Zhou, A. Shalimov, K. Potzger, N. M. Jeutter, C. Baehtz, M. Helm, J. Fassbender, and H. Schmidt, Appl. Phys. Lett. **95**, 192505 (2009).
[18] J. Bak-Misiuk, A. Misiuk, P. Romanowski, A. Barcz, R. Jakiela, E. Dynowska, J. Domagala, and W. Caliebe, Mater. Sci. Eng., B **159-160**, 99 (2009).
[19] A. Shalimov, K. Potzger, D. Geiger, H. Lichte, G. Talut, A. Misiuk, H. Reuther, F. Stromberg, S. Zhou, C. Baehtz, and J. Fassbender, J. Appl. Phys. **105**, 064906 (2009).
[20] F. Preisach, Z. Phys. **94**, 277 (1935).
[21] U. Gottlieb, A. Sulpice, B. Lambert-Andron, and O. Laborde, J. Alloys Compd. **361**, 13 (2003).
[22] W. Luo, S. R. Nagel, T. F. Rosenbaum, and R. E. Rosensweig, Phys. Rev. Lett. **67**, 2721 (1991).
[23] R. Sappey, E. Vincent, N. Hadacek, F. Chaput, J. P. Boilot, and D. Zins, Phys. Rev. B **56**, 14551 (1997).
[24] J. R. Friedman, U. Voskoboynik, and M. P. Sarachik, Phys. Rev. B **56**, 10793 (1997).
[25] R. K. Zheng, H. Gu, B. Xu, and X. X. Zhang, J. Phys.: Condens. Matter **18**, 5905 (2006).
[26] T. Song, R. M. Roshko, and E. D. Dahlberg, J. Phys.: Condens. Matter **13**, 3443 (2001).
[27] T. Song and R. M. Roshko, Physica B **275**, 24 (2000).
[28] Y. Park, S. Adenwalla, G. P. Felcher, and S. D. Bader, Phys. Rev. B **52**, 12779 (1995).
[29] Y. Sun, M. B. Salamon, K. Garnier, and R. S. Averback, Phys. Rev. Lett. **91**, 167206 (2003).
[30] M. Sasaki, P. E. Jonsson, H. Takayama, and H. Mamiya, Phys. Rev. B **71**, 104405 (2005).